Electronic Supplementary Material (ESI) for Dalton Transactions.

Electronic supporting information

Manganese-containing ionic liquids: synthesis, crystal structures and electrodeposition of manganese films and nanoparticles

Jeroen Sniekers, João Malaquias, Luc Van Meervelt, Jan Fransaer, Koen Binnemans*

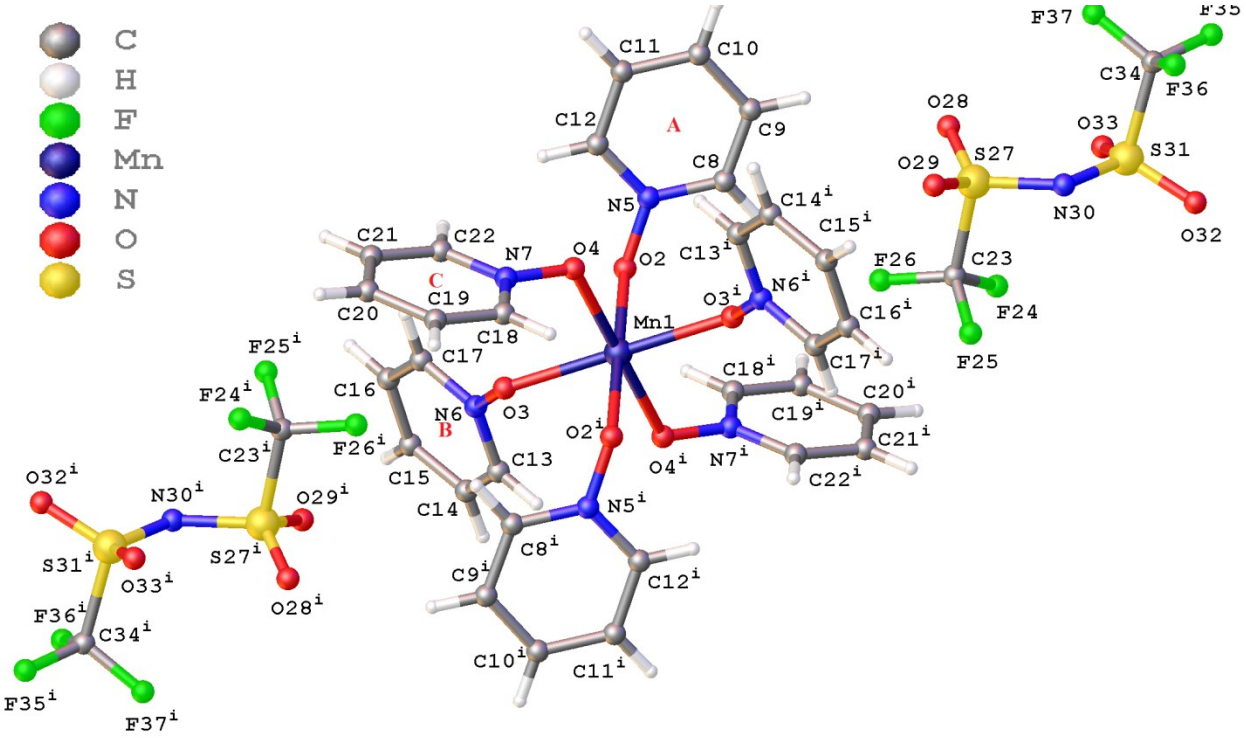

Figure S1: View of the crystal structure of $[Mn(py\text{-}O)_6][Tf_2N]_2$. Symmetry code: (i) 2-x, 1-y, 1-z.

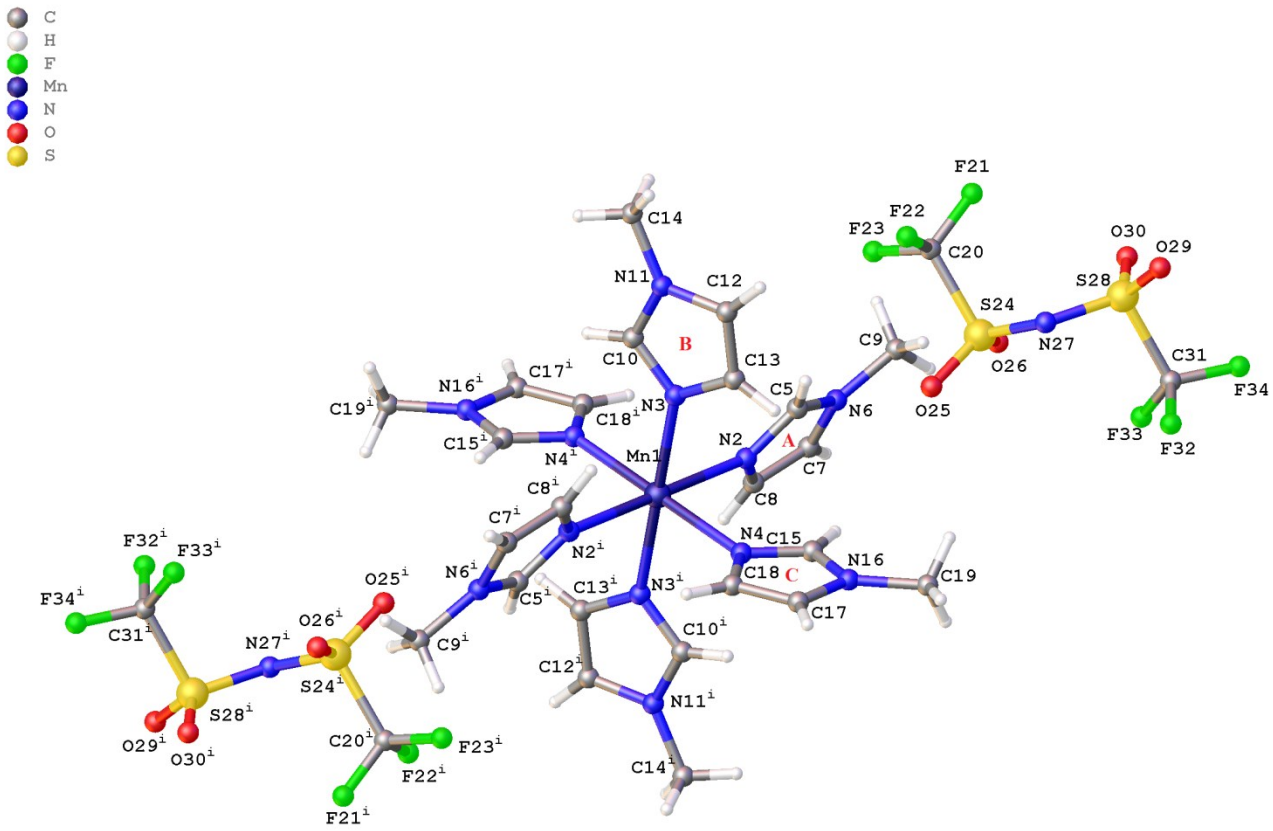

Figure S2: View of the crystal structure of $[Mn(MeIm)_6][Tf_2N]_2$. Symmetry code: (i) 1-x, 1-y, -z.

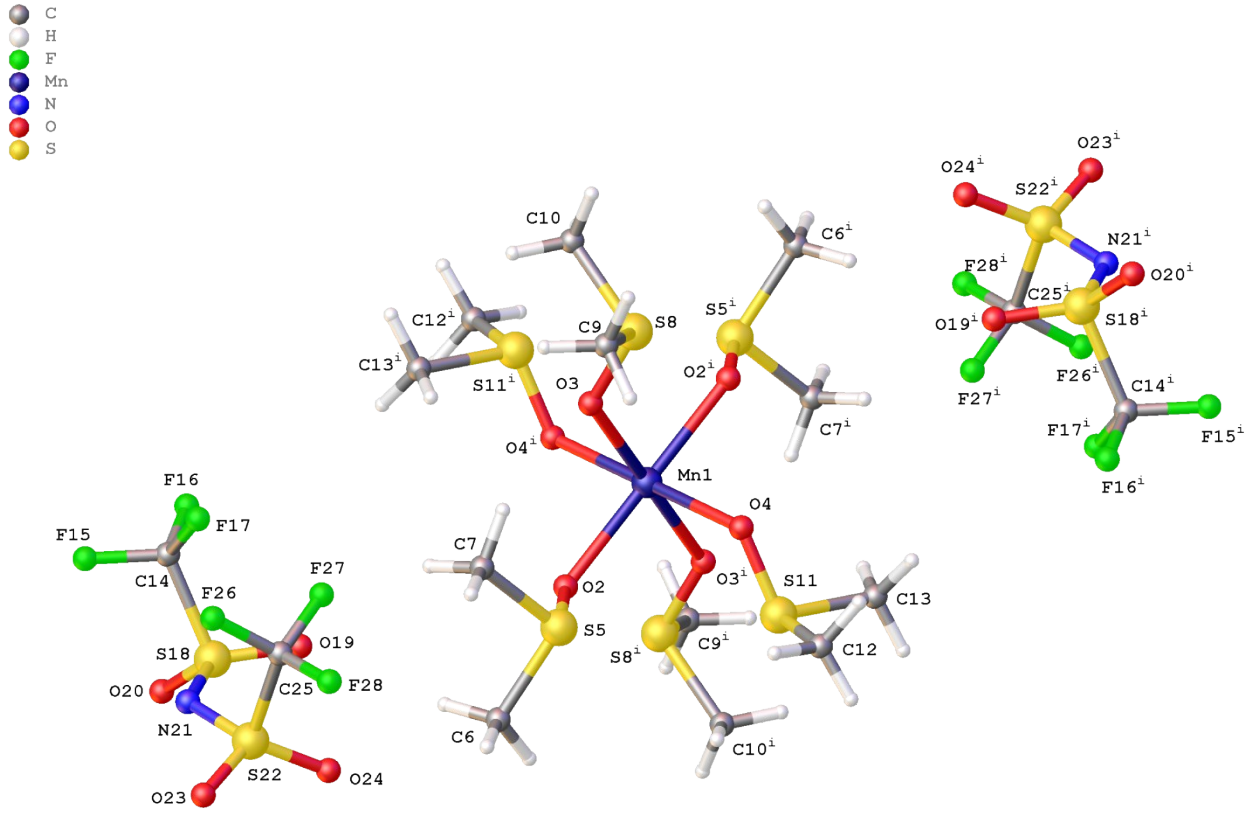

Figure S3: View of the crystal structure of $[Mn(DMSO)_6][Tf_2N]_2$. Symmetry code: (i) -x, -y, -z.

Table S1: Interatomic distances in all crystal structures.

Compound	X-Y···Z	Distance (Å)	Symmetry code Z	Compound	X-Y···Z	Distance (Å)	Symmetry code Z
$[Mn(py\text{-}O)_6][Tf_2N]_2$	C23-F26···ring C	3.337(2)	2-x, 1-y, 1-z	$Mn(Tf_2N)_2.6H_2O$	O2-H2A···O33	2.834(3)	1-x, 1-z, 1-z
	C34-F35···ring A	3.837(2)	1-x, 2-y1 1-z		O2-H2B···O14	3.130(4)	1-x, 1-z, 1-z
	C34-F35···ring C	3.372(3)	1-x, 1-y, 1-z		O2-H2B···N15	3.052(3)	1-x, 1-z, 1-z
	C34-F37···ring A	3.703(3)	1-x, 2-y, 1-z		O3-H3A···O32	2.817(3)	
	S27-O29···ring B	3.234(3)	2-x, 1-y, 1-z		O3-H3B···N30	2.966(3)	1-x, 1-y, -z
	C8-H8···F26	3.243(4)			O4-H4A···O17	2.799(3)	1-x, 1-y, 1-z
	C9-H9···O28	3.449(5)			O4-H4B···O29	2.880(3)	1-x, 1/2+y, 1/2-z
	C12-H12···O32	3.343(4)	1/2+x, 3/2-y, -1/2+z		O5-H5A···O28	2.895(3)	1-x, 1-y, -z
	C14-H14···O28	3.393(4)	1+x, y, z		O5-H5B···O18	2.762(3)	-x, 1-y, 1-z
	C15-H15···O28	3.325(4)	2-x, 1-y, 1-z		O6-H6A···O28	2.857(3)	
	C17-H17···O32	3.318(4)	1/2+x, 3/2-y, -1/2+z		O6-H6B···O29	2.918(3)	1-x, -1/2+y, 1/2-z
	C19-H19···O2	3.180(4)	x, -1+y, z		O6-H6B···O33	2.887(3)	1-x, 1-y, 1-z
	C20-H20···N30	3.454(5)	1/2+x, 1/2-y, -1/2+z		O7-H7A···O14	2.828(4)	1-x, 1-y, 1-z
	C22-H22···O32	3.284(4)	1/2+x, 3/2-y, -1/2+z		O7-H7B···O13	2.737(4)	-x, 1-y, 1-z
$[Mn(MeIm)_6][Tf_2N]_2$	C20-F21···ring A	3.4462(15)	1-x, 1/2+y, 1/2-z	$[Mn(G_3)_1][Tf_2N]_2$	C5-H5A···O17	3.219(17)	1-x, 1-y, z
	C31-F32···ring A	3.5615(16)	1-x, -1/2+y, 1/2-z		C6-H6A···F21	3.475(18)	5/4-x, 1/4+y, 1/4+z
	C31-F33···ring B	3.4571(16)	1-x, -1/2+y, 1/2-z	$[Mn(G_2)_1][OTf]_2$	C8-H8A···F17	3.159(3)	x, -1+y, z
	C7-H7···O25	3.247(2)	1+x, y, z		C8-H8B···O14	3.195(3)	1-x, -1/2+y, 1/2-z
	C9-H9···O26	3.328(3)			C10-H10A···O13	3.452(3)	1-x, 1-y, 1-z
	C17-H17C···O29	3.282(2)	-x, -1/2+y, 1/2-z		C11-H11A···O14	3.275(3)	x, 3/2-y, 1/2+z
	C19-H19A···O26	3.336(3)	1-x, -1/2+y, 1/2-z		C11-H11B···O21	3.503(3)	2-x, 1-y, 1-z
	C19-H19B···O29	3.373(3)	-x, -1/2+y, 1/2-z	$Mn(OTf)_4(H_2O)_4.(G_2)_2$	O2-H2A···O3	2.928(3)	1/2+x, 1/2-y, 1/2-z
$[Mn(DMSO)_6][Tf_2N]_2$	C6-H6A···O19	3.369(3)			O2-H2B··O12	2.765(3)	-1/2+x, 1/2-y, 1/2-z
	C6-H6C···O20	3.383(3)	1-x, 1-y, -z		O3-H3A··O15	2.705(2)	-1+x, y, z
	C7-H7A···O3	3.358(4)			O3-H3B··O15	2.705(2)	-1+x, 1/2-y, z
	C7-H7C···O19	3.422(3)			C13-H13B··O15	3.490(3)	-1/2+x, y, 3/2-z
	C9-H9B···O23	3.299(3)	-1+x, -1+y, z		C14-H14A··O6	3.350(3)	
	C12-H12C···O19	3.454(4)	1+x, y, z				
	C13-H13B···O23	3.538(3)	-x, 1-y, -z				
	C13-H13C···O4	3.532(3)	-1-x, -y, -z				

Table S2: Crystal data and structure refinement for the structures of $[Mn(py\text{-}O)_6][Tf_2N]_2$, $[Mn(MeIm)_6][Tf_2N]_2$, $[Mn(DMSO)_6][Tf_2N]_2$,$Mn(Tf_2N)_2{\cdot}H_2O$, $[Mn(G_3)_1][Tf_2N]_2$, $[Mn(G_2)_1][OTf]_2$ and $Mn(OTf)_4(H_2O)_4{\cdot}(G_2)_2$.

	$[Mn(py\text{-}O)_6][Tf_2N]_2$	$[Mn(MeIm)_6][Tf_2N]_2$	$[Mn(DMSO)_6][Tf_2N]_2$	$Mn(Tf_2N)_2.6H_2O$	$[Mn(G_3)_1][Tf_2N]_2$	$[Mn(G_2)_1][OTf]_2$	$Mn(OTf)_4(H_2O)_4.(G_2)_2$
Empirical Formula	$C_{34}H_{30}F_{12}MnN_8O_{14}S_4$	$C_{28}H_{36}F_{12}MnN_{14}O_8S_4$	$C_{16}H_{36}F_{12}MnN_2O_{14}S_{10}$	$C_4H_{12}F_{12}MnN_2O_{14}S_4$	$C_{12}H_{18}F_{12}MnN_2O_{12}S_4$	$C_{16}H_{28}F_{12}Mn_2O_{18}S_4$	$C_8H_{18}F_6MnO_{11}S_2$
CCDC number	1511760	1511764	1511765	1511766	1511761	1511762	1511763
Formula weight	1185.84	553.94	1081.01	723.36	793.46	487.25	523.28
Temperature/K	99.97(11)	100.0(3)	100.0(3)	100.01(10)	100(2)	99.9(4)	100.0(3)
Color	transparent	transparent	transparent	transparent	transparent	transparent	transparent
Size/mm³	0.08 x 0.05 x 0.04	0.09 x 0.07 x 0.04	0.03 x 0.02 x 0.02	0.24 x 0.16 x 0.09	0.19 x 0.17 x 0.09	0.12 x 0.08 x 0.06	0.15 x 0.06 x 0.06
Space group	$P2_1/n$	$P2_1/c$	P-1	$P2_1/c$	Fdd2	$P2_1/c$	Pnma
a/Å	12.8101(9)	8.3943(3)	8.0015(6)	10.4969(4)	39.801(2)	13.6419(2)	9.6566(3)
b/Å	8.4090(4)	11.1474(5)	10.9806(9)	23.2549(14)	15.0805(11)	9.97668(13)	20.1455(9)
c/Å	21.9978(10)	24.3863(9)	12.9203(8)	10.2815(4)	8.9654(5)	13.8425(2)	10.0161(4)
α/Å	90	90	109.047(7)	90	90	90	90
β/Å	99.280(5)	97.523(4)	99.445(6)	90.464(4)	90	105.4760(16)	90
γ/Å	90	90	97.393(6)	90	90	90	90
Volume/Å³	2338.6(2)	2262.29(16)	1038.09(14)	2509.7(2)	5381.2(5)	1815.67(5)	1948.51(12)
Z	2	2	1	4	8	2	4
ρ_{calc} Mg/m³	1.684	1.626	1.734	1.914	1.959	1.782	1.784
μ/mm^{-1}	0.580	0.587	0.930	1.006	0.943	1.054	0.996
Wavelength/Å	0.71073	0.71073	0.71073	0.71073	0.71073	0.71073	0.71073
Reflections collected	9867	9993	7448	20230	3703	7750	7558
Independent reflections	4770	4626	4225	5116	2202	3706	2045
R(int)	0.0563	0.0327	0.0343	0.0369	0.0773	0.0306	0.0359
R_1 [I≥2σ(I)]	0.0692	0.0385	0.043	0.0404	0.0777	0.0357	0.0411
wR_2 [all data]	0.1524	0.0789	0.0799	0.0762	0.1802	0.0741	0.0923

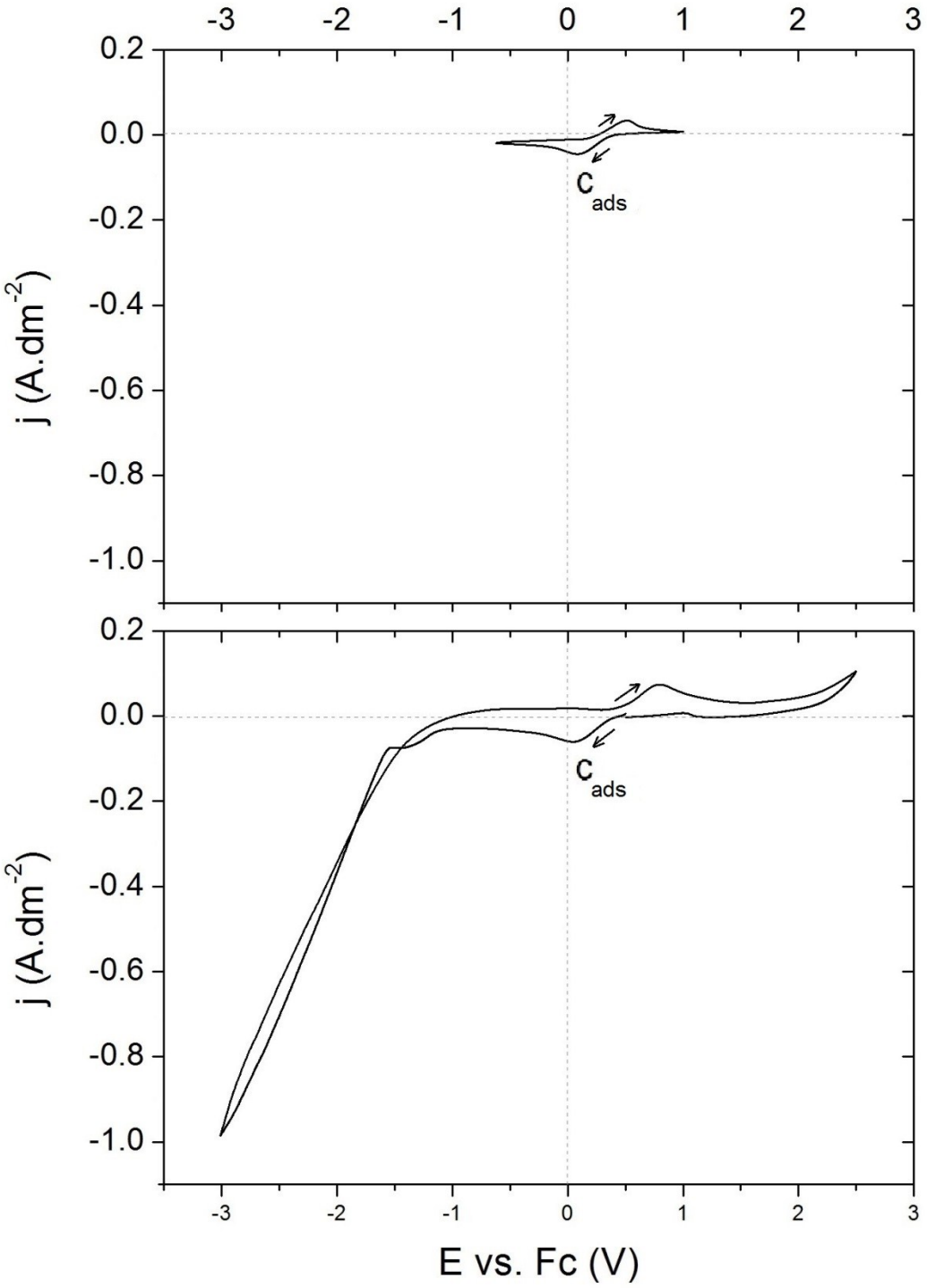

Figure S4: Cyclic voltammograms of $[Mn(G_3)_1][Tf_2N]_2$ on a Pt-coated silicon wafer working electrode. Top: scan range -0.6 V to +1.0 V vs Fc to show the process related to the bistriflimide anion; bottom: scan range -3.0 V to +2.5 V to show the bulk manganese metal deposition as well as the start of the anodic degradation of the ligand. The scans were recorded with v_{scan} = 30 mV s^{-1} and at T = 120 °C, a manganese plate was used as counter electrode and ferrocene/ferrocenium in $[BMP][Tf_2N]$ as reference electrode.

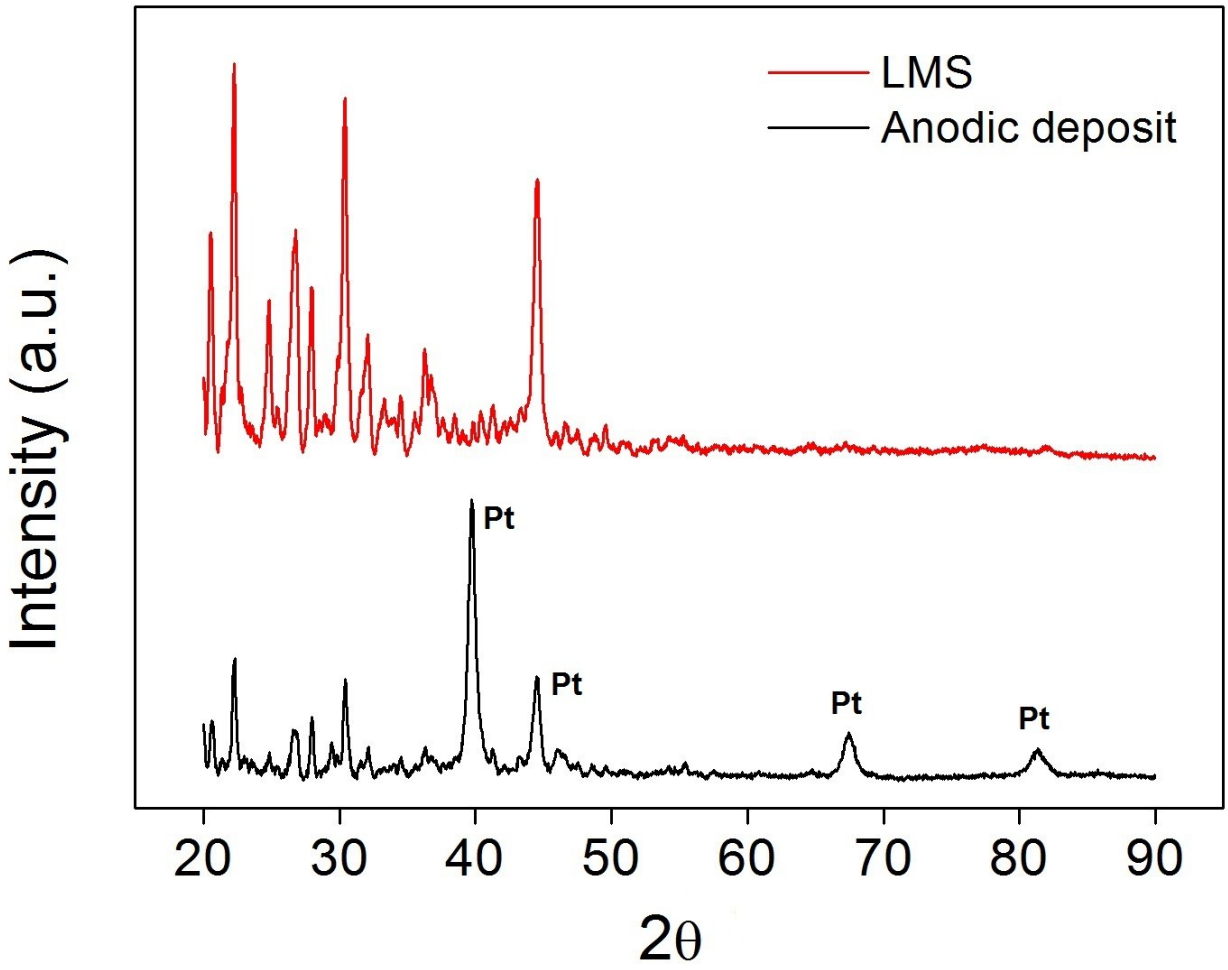

Figure S5: Grazing incidence X-Ray Diffraction pattern from the anodic deposit formed at +1.2 V vs Fc^+/Fc in $[Mn(py\text{-}O)_6][Tf_2N]_2$ compared to that of pure $[Mn(py\text{-}O)_6][Tf_2N]_2$.

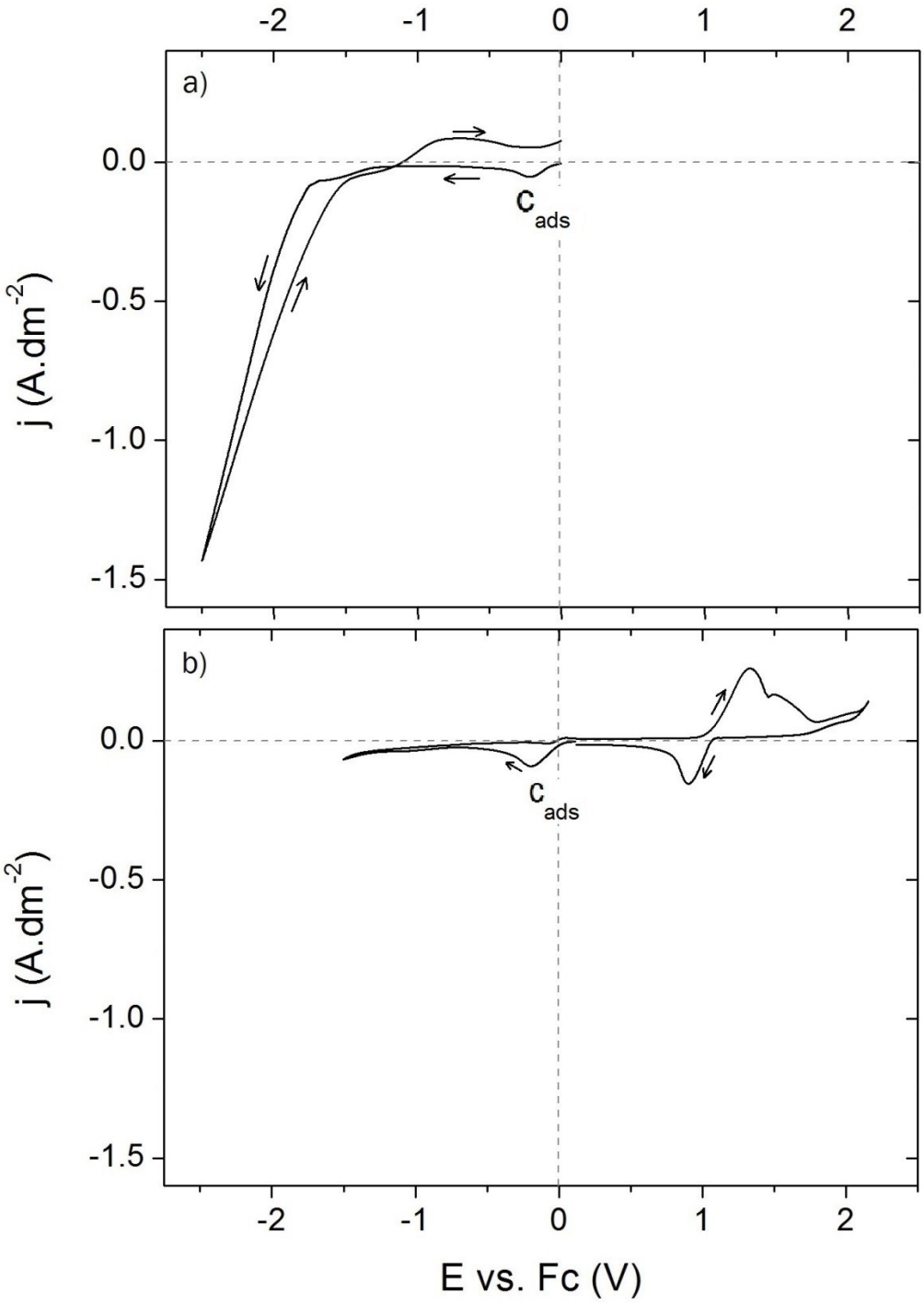

Figure S6: Cyclic voltammograms of $[Mn(DMSO)_6][Tf_2N]_2$ on a Pt-coated silicon wafer working electrode. Top: scan range 0.0 V to -2.5 V vs Fc to show the process related to the bistriflimide anion and the bulk deposition of manganese metal; bottom: scan range +2.25 V to -1.6 V to show the Mn^{3+}/Mn^{2+} redox couple as well as the start of the anodic degradation of the ligand. The scans were recorded with v_{scan} = 30 mV s^{-1} and at T = 120 °C, a manganese plate was used as counter electrode and ferrocene/ferrocenium in $[BMP][Tf_2N]$ as reference electrode.

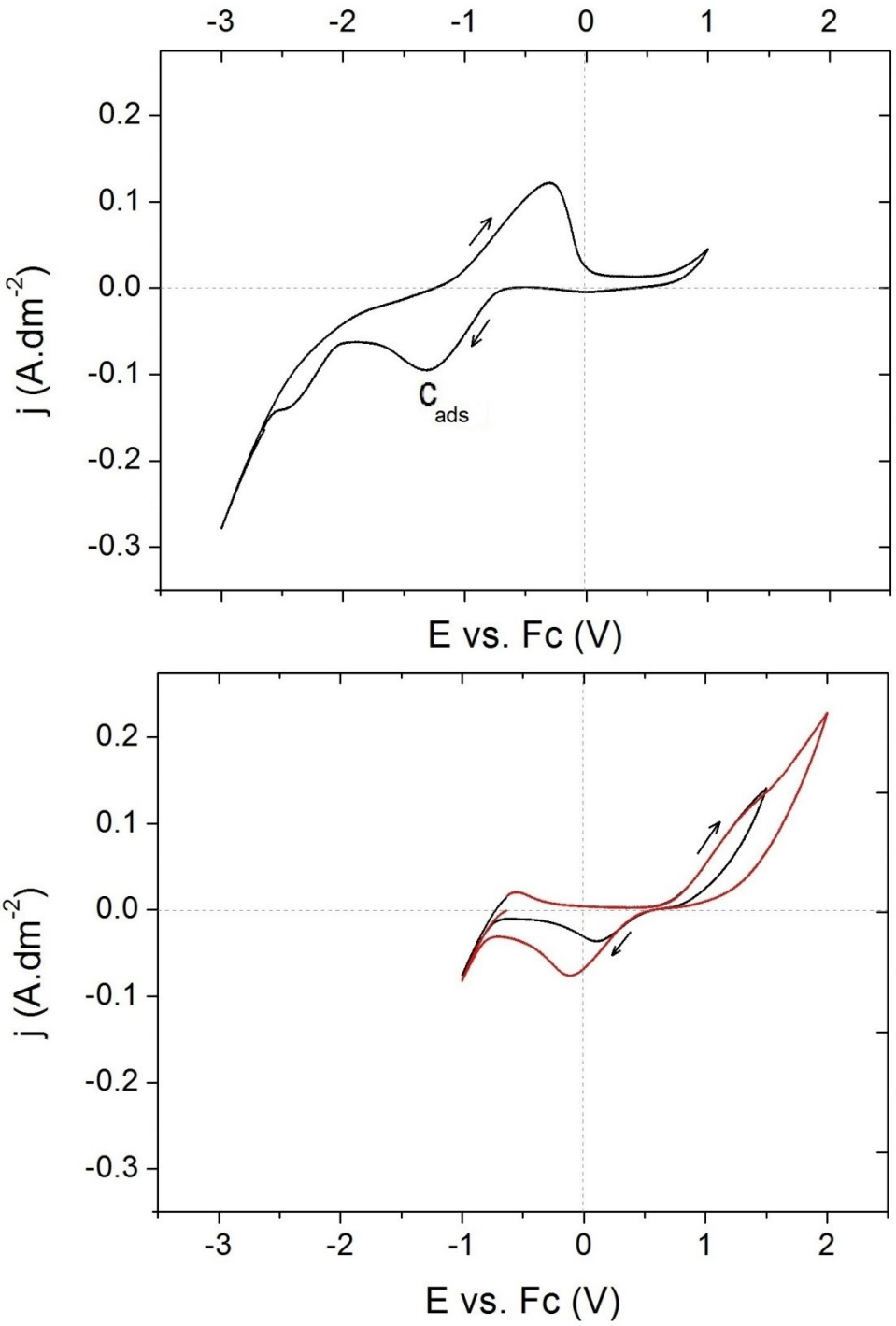

Figure S7: Cyclic voltammograms of $[Mn(HeIm)_6][Tf_2N]_2$ on a Pt-coated silicon wafer working electrode. Top: scan range -3.0 V to +1.0 V vs Fc to show the reduction to manganese metal as well as the small cathodic process related to the bistriflimide anion; bottom: scan range -1.0 V to +2.0 V vs Fc to show the quasi-reversible Mn^{3+}/Mn^{2+} redox couple. Bottom scan is started in anodic direction. The scans were recorded with v_{scan} = 30 mV s^{-1} and at T = 120 °C, a manganese plate was used as counter electrode and ferrocene/ferrocenium in $[BMP][Tf_2N]$ as reference electrode.

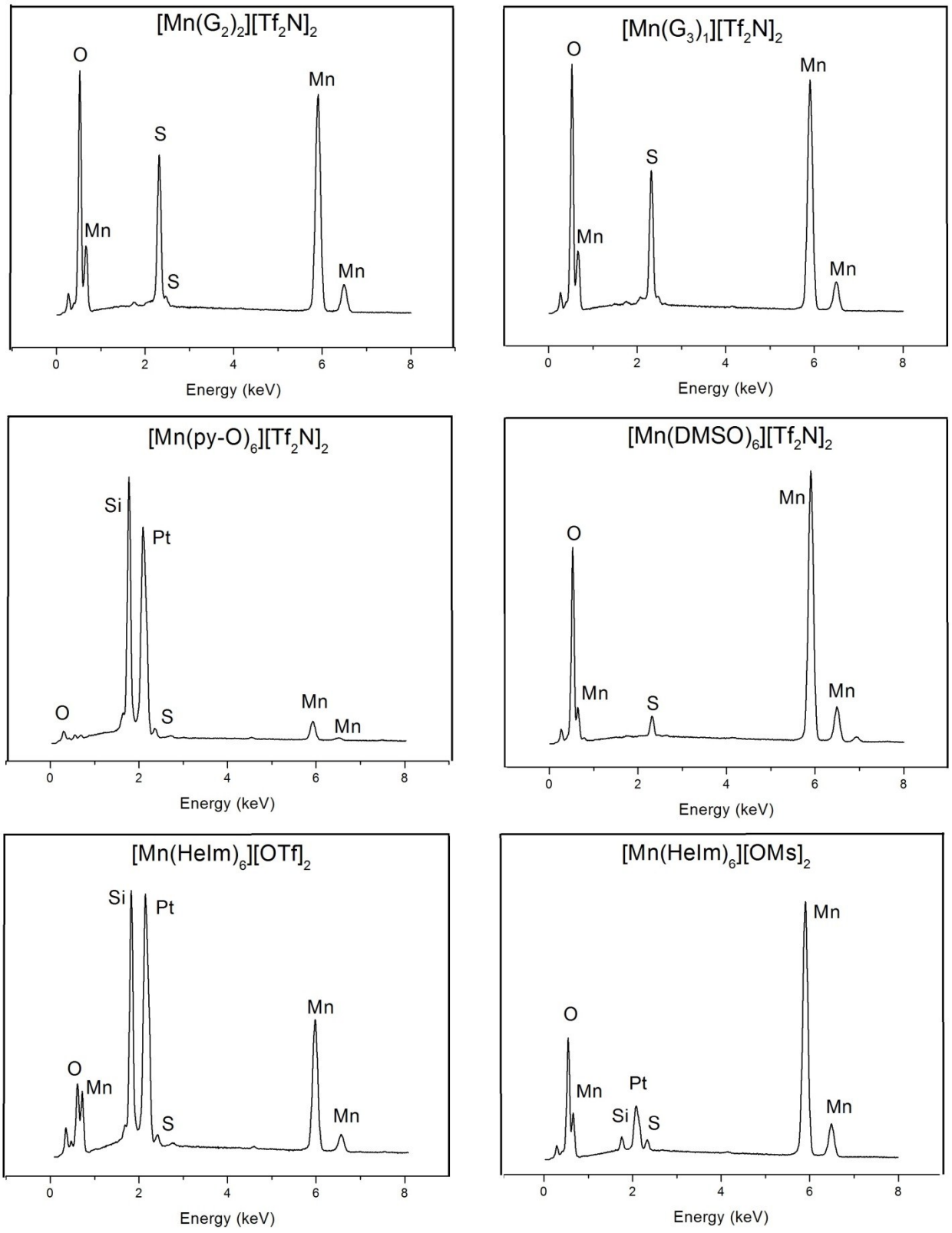

Figure S8: EDX spectra of the deposits obtained by electrodeposition from $[Mn(DMSO)_6][Tf_2N]_2$. $[Mn(G_2)_2][Tf_2N]_2$. $[Mn(G_3)_1][Tf_2N]_2$ and $[Mn(py\text{-}O)_6][Tf_2N]_2$.